Ratiometric Coumarin – Neutral Red (CONER) Nanosensor for Detection of Hydroxyl Radicals

Gabriela M. Ganea[1], Paulina E. Kolic[1], Bilal El-Zahab[1], and Isiah M. Warner[1*]

[1]Department of Chemistry, Louisiana State University, Baton Rouge, Louisiana, 70803

[*] Address: Department of Chemistry, 434 Choppin Hall, Louisiana State University, Baton Rouge, 70803 LA, United States; Tel.: +1 225 5782829; Fax: +1 225 5783971; e-mail address: iwarner@lsu.edu

Synthesis of Coumarin Functionalized Molecular Micelles

The synthesis scheme for C3C-poly-Nε-SUK is presented in Scheme S1. The amino acid based molecular micelle poly (sodium *N*-undecylenyl-Nε-Boc lysinate) (poly- Nε-Boc-SUK) was synthesized according to the procedure described by Macossay *et al.*[1] The deprotection of Boc group was achieved in a mixture of DCM and TFA 1:1 v/v for 4 hours at room temperature. In the first step the carboxylic group of C3C was activated with DCC/NHS, resulting in the succinimidyl ester of C3C (SECCA), according to an modified procedure described by Bardajee et al.[2] The unprotected poly-Nε-SUK (100 mg) was dissolved in sodium carbonate 0.1 M (5mL) followed by the addition of SECCA dissolved in 1:4 v/v DMSO:DMF (5 mL) and allowed to react overnight. The solvent was removed by dialysis (cellulose ester membrane, MWCO 1000 Da, Spectrum Laboratories, Inc., Rancho Dominguez, CA, USA) for 24 hours. The final product, C3C-poly-Nε-SUK, was freeze-dried and refrigerated. Proton NMR indicated the completion of the coupling reaction by the presence of coumarin chemical shifts in the 7-9 ppm region (^{1}H NMR (400 MHz, D_2O): δ8.54 (s), 8.29 (s), 7.79 – 7.59 (m), 7.39 (dd), 7.09 (s), 4.80 (s), 4.22 (s), 3.32 (s), 2.65 (s), 2.41 (s), 1.88 (s), 1.58 (s), 1.41 (s), 1.03 (s)).

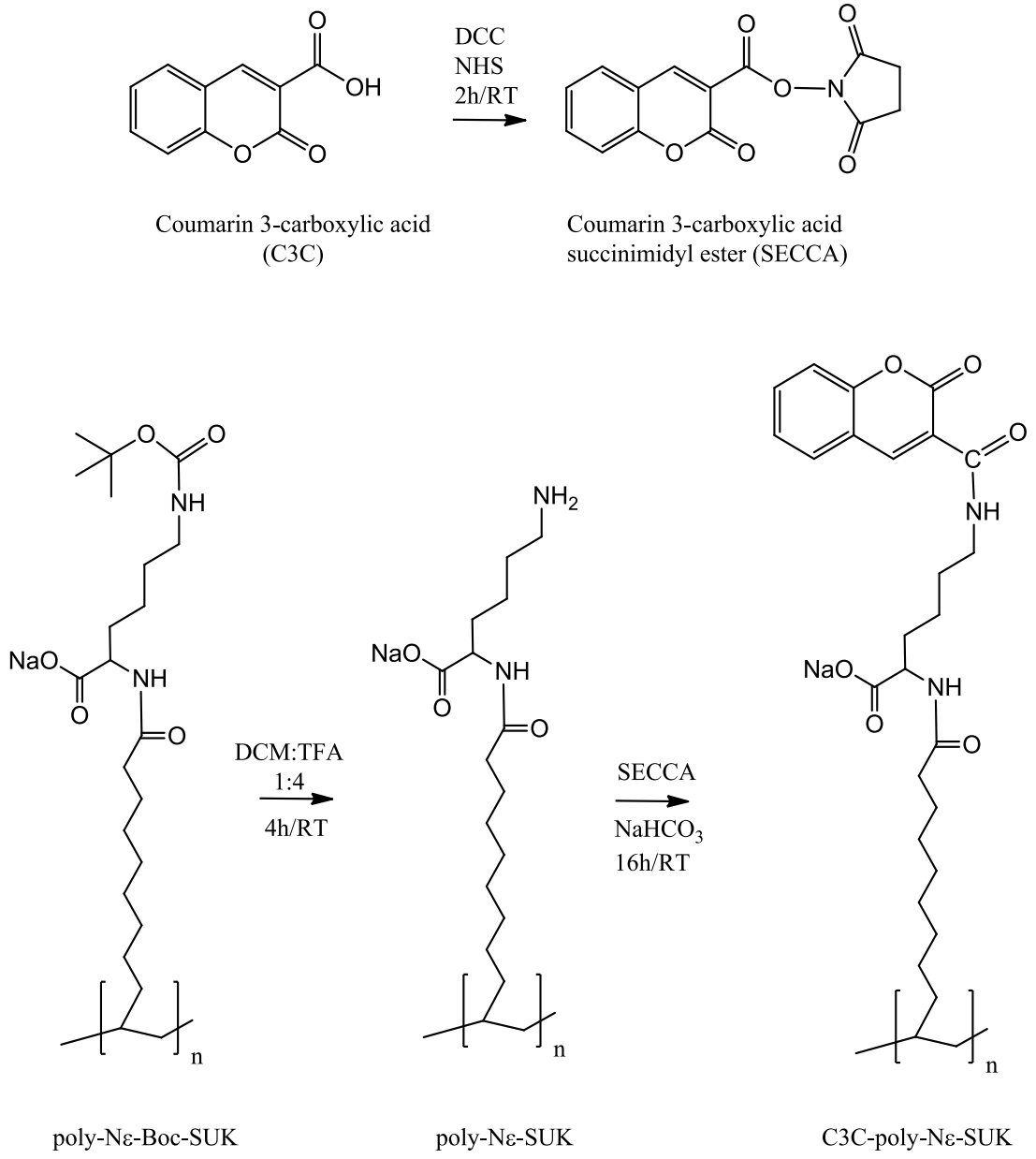

Scheme S1. Synthesis of C3C-poly-Nε-SUK micelle.

Effect of Reaction Time

In general, hydroxyl radicals have a short life-time in solution and rapidly react with surrounding molecules. Due to sample preparation and instrumental limitation, the time needed

for nanoparticle reaction with $OH^{\bullet}$ radicals was established by stopping the reaction at various time intervals using DMSO as $OH^{\bullet}$ scavenger. DMSO rapidly reacts with hydroxyl radicals and likely eliminates their presence in solution. In Figure S1 the I_{450}/I_{528} ratio between C3C fluorescence intensity at 450 nm and NeR fluorescence intensity at 528 nm is represented as a function of time.

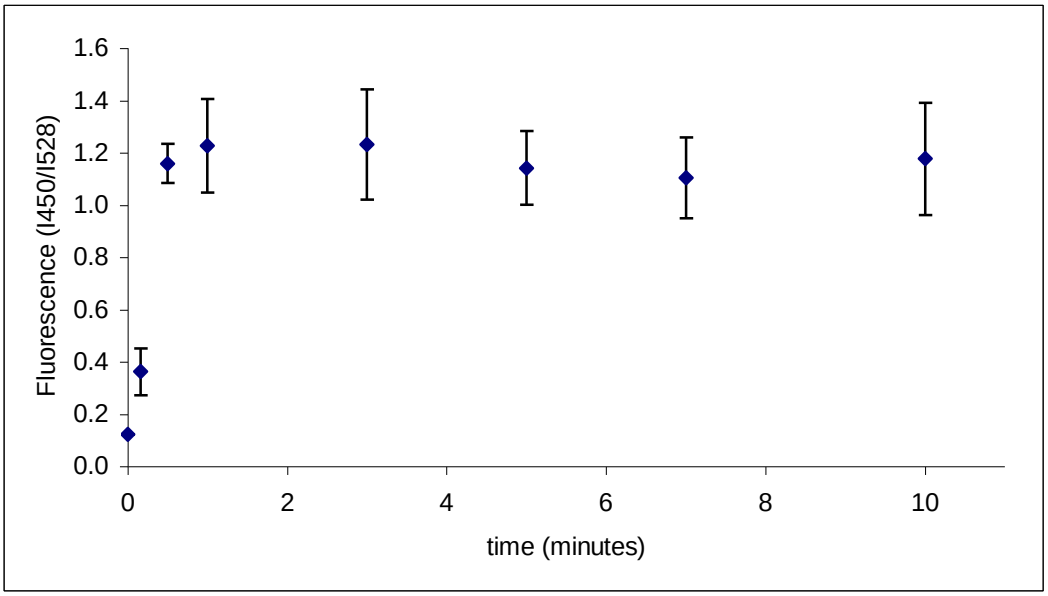

Figure S1. Effect of reaction time on fluorescence ratio after the reaction of nanoparticles with $OH^{\bullet}$ (0.07 mg/mL nanoparticles, 200 μM $CuSO_4$, 20 mM H_2O_2 and 200 μM ascorbic acid; total volume 500 mL).

A linear increase of I_{450}/I_{528} is observed in the first minute, indicating that the radicals were rapidly consumed in the reaction with C3C. It is worth mentioning that the reaction of $OH^{\bullet}$ with C3C is irreversible, and limited by the concentration of radicals. After one minute, it is possible that $OH^{\bullet}$ radical concentration decreased. Therefore, further increase in the fluorescent ratiometric signal was not observed with increase in the reaction time. For further experiments, the reaction was stopped at 5 minutes in order to ensure the complete reaction.

Effect of Nanoparticle Concentration

Spectroscopic analyses using nanoparticle reactions with various molecules were limited by scattering effects. Therefore, nanoparticle concentration was kept minimal within the instrumental limitations. Figure S1 represents the fluorescence spectra of increasing concentrations of nanoparticle suspensions that were exposed to the same concentration of $OH^{\bullet}$ radicals.

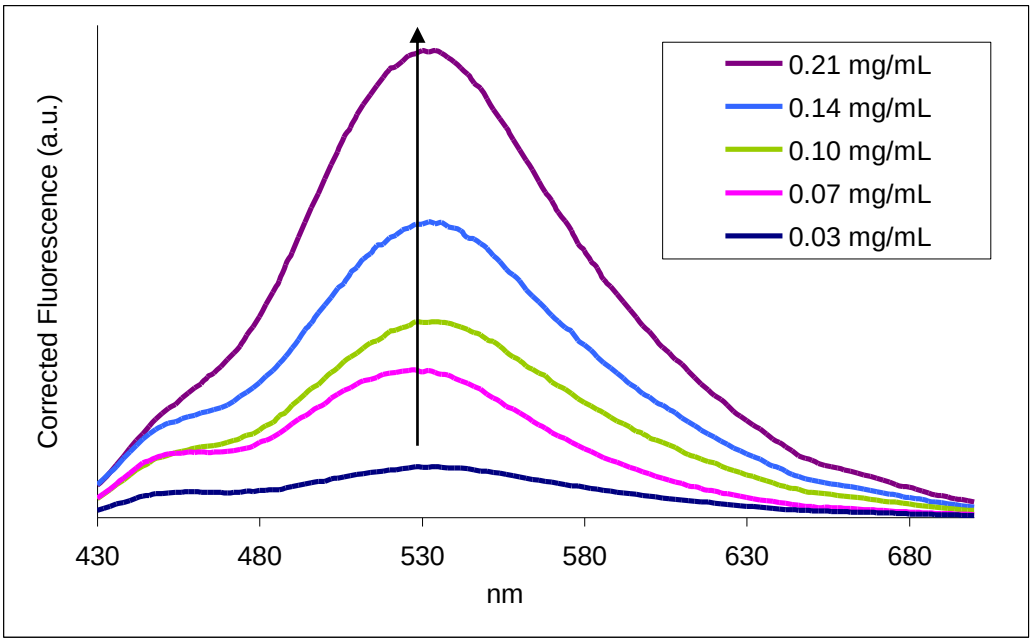

Figure S2. Fluorescence spectra of nanoparticles at various concentrations after the reaction with $OH^{\bullet}$.

It is noteworthy that the intensity of the NeR peak increased with the increase in nanoparticle concentration. However, as more nanoparticles were used in the reaction, the peak corresponding to 7-OH C3C started to become less pronounced. Since the concentration of $OH^{\bullet}$ radicals remained constant, an increase in nanoparticle concentration did not produce an increase of 7-OH peak. However, it resulted in an increase of only NeR peak. In addition, cloudiness in the

reaction medium was observed at concentrations exceeding 0.1 mg/mL. A concentration of 0.07 mg/mL nanoparticles was found to be optimum for the presented ratiometric experiments.

Effect of Coumarin Location

The fluorescence spectra of C3C-poly-Nε-SUK modified NeR-loaded PLGA nanoparticles and poly-Nε-Boc-SUK modified NeR/SECCA-loaded PLGA nanoparticles are shown in Figure S3. Poly-Nε-Boc-SUK modified NeR/SECCA-loaded PLGA nanoparticles were obtained by co-encapsulation of succinimidyl ester of C3C (SECCA) and NeR in the polymeric core. As expected, the spectrum for CONER sensors contained both signals from reporting and reference dyes, respectively (Figure S3, graph a). In contrast, the nanoparticles containing both SECCA and NeR within the polymer matrix presented only one peak in the fluorescence spectrum likely due to NeR fluorescence. In addition, no evident intensity of 7-OH C3C was observed (Figure S3, graph b) indicating that C3C was likely shielded by the polymeric matrix and therefore not readily available for the reaction with hydroxyl radicals. Such results suggested that the presence of coumarin moiety on the surface of the nanoparticles was relevant for the design and use of CONER sensors for the detection of $OH^{\bullet}$ radicals.

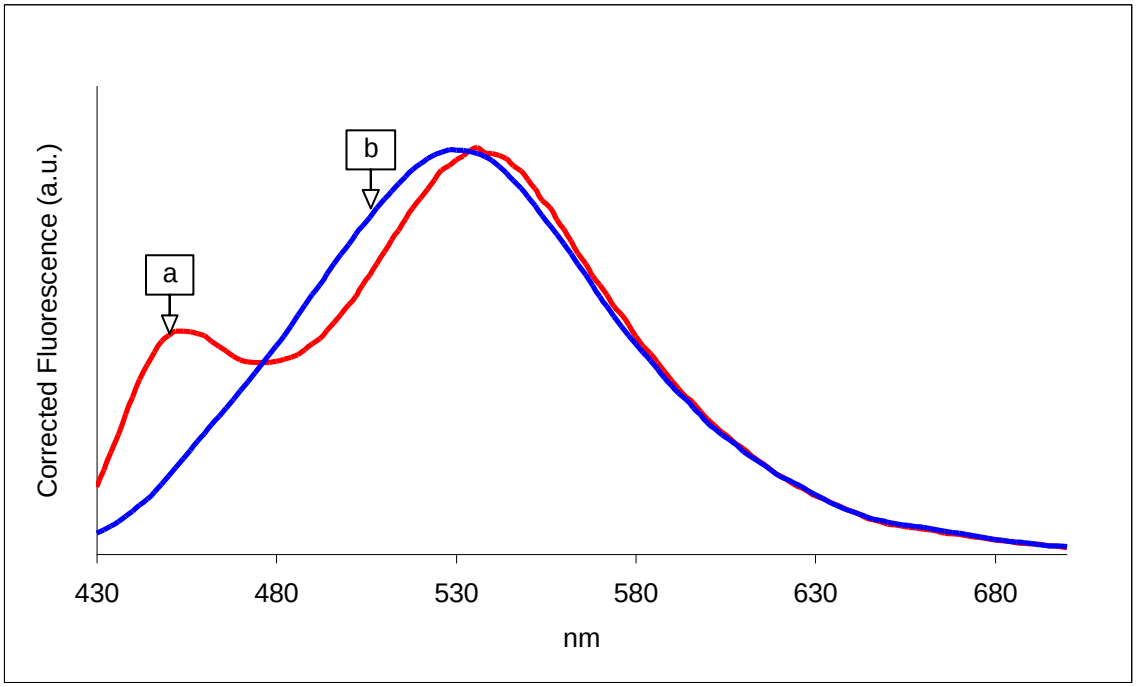

Figure S3. Corrected fluorescence of nanoparticles after the reaction with $OH^{\bullet}$ a) C3C-poly-Nε-SUK-modified NeR-loaded nanoparticles; b) poly-Nε-Boc-SUK NeR/SECCA-loaded nanoparticles.

Effect of hydroxyl radical concentration

The I_{450}/I_{528} was calculated as the ratio between C3C fluorescence intensity at 450 nm and NeR fluorescence intensity at 528 nm. The I_{450}/I_{528} ratio was represented as a function of $OH^{\bullet}$ concentration (as μM $CuSO_4$) in Figure S4 on a logarithmic scale. It was observed that the fluorescence intensity ratio increased as the concentration $OH^{\bullet}$ radicals increased up to approximately 50 μM $CuSO_4$. Using the linear region of the graph, a limit of detection of 0.73 μM $OH^{\bullet}$ was calculated. As the $OH^{\bullet}$ concentration further increased, it was observed that the logarithmic value of I_{450}/I_{528} ratio decreased likely due to reaction saturation and decrease in the production of 7-OH C3C fluorescent product.

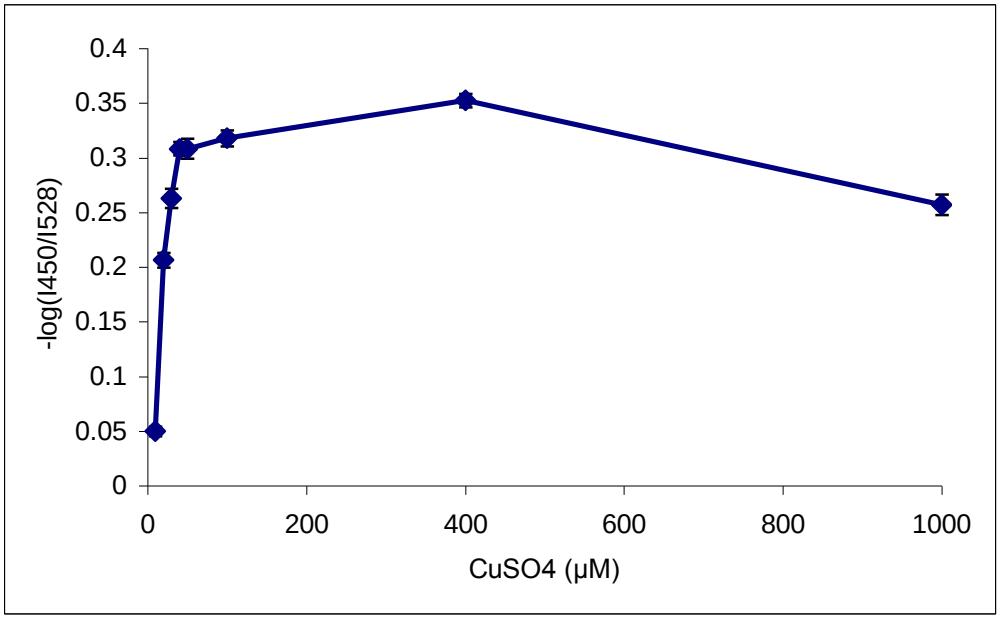

Figure S4. Logarithmic I450/I528 ratio as a function of $CuSO_4$ concentration.

In vitro Detection of Hydroxyl Radicals

Several control experiments were performed in order to verify the change in fluorescence signal in the cells exposed to oxidative stress. The cells were investigated in the absence of nanoparticles (Figure S5, a) and b)). It was noticed that the cells presented weakly green autofluorescence likely due to natural cell components or other compounds resulted from non specific reactions of hydroxyl radicals with cellular components. However, such signal was significantly lower than the signal obtained for cells incubated with CONER sensors. The cells were incubated with nanoparticles containing only C3C moiety (Figure S5, c) and d)) as well as nanoparticles containing only NeR (Figure S5, e) and f)). It was observed that the cells did not change their appearance in absence of NeR and no red color was observed. Similarly, in the absence of C3C the cells appeared red before and after exposure to oxidative stress.

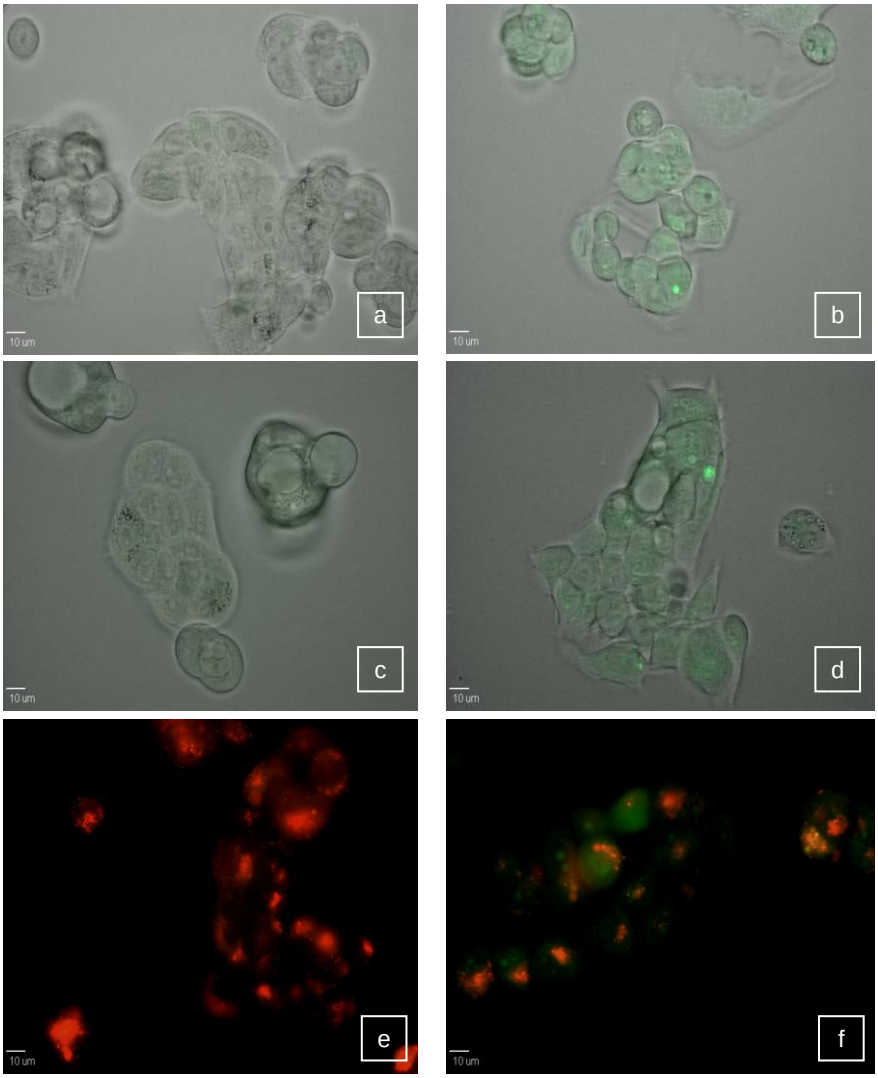

Figure S5. Cells in the absence of nanoparticles a) before H_2O_2 treatment, b) after H_2O_2 treatment; cells incubated with nanoparticles containing only C3C c) before H_2O_2 treatment, d) after H_2O_2 treatment; cells incubated with nanoparticles containing only NeR e) before H_2O_2 treatment, f) after H_2O_2 treatment.

References

1 Macossay, J.; Shamsi, S. A.; Warner, I. M. *Tetrahedron Letters* **1999**, *40*, 577-580.

2 Bardajee, G. R.; Winnik, M. A.; Lough, A. J. *Acta Crystallographica Section E-Structure Reports Online* **2007**, *63*, o1513-o1514.